Journal of Materials Chemistry A

Accepted Manuscript

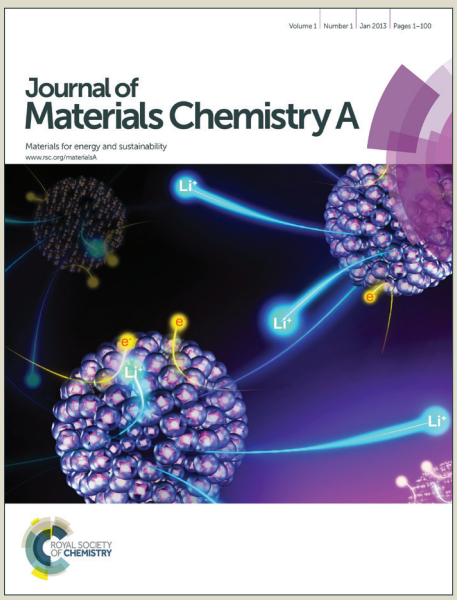

ROYAL SOCIETY OF CHEMISTRY

www.rsc.org/materialsA

Highly compressible and stretchable superhydrophobic coating inspired by bio-adhesion of marine mussels

Fatang Liu, Fenghe Sun, Qinmin Pan*

(School of Chemical Engineering and Technology, Harbin Institute of Technology, Harbin, 150001, *P. R.* China)

Corresponding author:

Qinmin Pan

School of Chemical Engineering and Technology

Harbin Institute of Technology, Harbin 150001, People's Republic of China

E-mail: panqm@hit.edu.cn

Abstract

Mechanical durability is an important issue for the fabrication and application of superhydrophobic coatings, but rare studies reported such a coating could withstand both large-strain compression and stretching. In this study, a highly compressible and stretchable superhydrophobic coating was constructed on the surface of commercial polyurethane (PU) sponges, inspired by the bio-adhesion of marine mussels. The coating consisted of sandwich-like multilayers constructed through layer-by-layer deposition of polydopamine (PDA) films and Ag nanoparticles. Under large strain conditions, the resulting coating could withstand 6000-cycle compressions, as well as 2000-cycle tensile measurements without losing superhydrophobicity, exhibiting outstanding mechanical robustness among the existing counterparts. The mechanism for the high compressibility and stretchability is believed to arise from the strong interactions between silver nanoparticles, PDA interlayers and sponge skeletons. Additionally, the coating also exhibited excellent anti-icing property at −15 ^{o}C. Because of simple synthesis process and almost nonselective adhesion of PDA, the results might provide a facile and versatile route to fabricate mechanically robust coatings on elastic substrates for various technological applications.

Keywords: mussel-inspired; superhydrophobic coating; polydopamine/Ag multilayers; high compressibility; high stretchability; anti-icing

1. Introduction

Superhydrophobic surfaces (water contact angle greater than 150^{o}) had attracted much interest in both scientific and industrial communities.[1,2] Nevertheless, most of the reported superhydrophobic surfaces exhibited poor durability against mechanical stress and thus impeding their practical applications.[3,4] In the past years, several strategies were proposed to improve the mechanical robustness of superhydrophobic surfaces, such as cross-linking of superhydrophobic coatings,[5-8] forming covalent bonding between superhydrophobic coatings and substrates,[9-12] introducing elastomeric nanocomposite,[13] protective mircopillars,[14] as well as self-healing capability, *etc*.[15-19] Indeed, most of these methods effectively enhanced the durability of superhydrophobic surfaces against machine washing, [6,9,10,13,15] abrasion,[6-9,11-16,18,19] even the damage caused by icing.[20-22] However, there is a lack of robust superhydrophobic coatings that can withstand both large-strain compression and stretching. Considering wide applications in daily life and technological fields, it is important to construct a highly compressible and stretchable superhydrophobic coating through a facile strategy. The challenge for such a coating requires not only flexibility, but also reversible deformation under large strain without collapse.

Generally, improving the adhesion (or interactions) between hierarchical topologies and substrates is crucial for the mechanical durability of superhydrophobic coatings.[3,6] In this regard, marine mussels might provide us an alternative inspiration to achieve this goal. In nature, mussels adhere to most organic and inorganic surfaces under wet conditions by secreting adhesive proteins that contain high content of 3,4-dihydroxyphenylalanine (DOPA).[23-25] Further studies revealed that dopamine and its analogues (*i.e*., catecholic moieties) presented in DOPA are main components responsible for the strong adhesion of mussels.[26-28] All these findings motivate us to enhance the mechanically durability of a superhydrophobic coating by using strong adhesive properties of catecholic moieties.

Taking inspiration from mussel adhesion, herein, we constructed a highly compressible and stretchable superhydrophobic coating on commercial polyurethane (PU) sponge through layer-by-layer deposition[29,30] of

polydopamine (PDA) films and Ag nanoparticles (Scheme 1). Under large strain conditions, the resulting sandwich-like coating withstood 6000-cycle compressions and 2000-cycle tensile tests without losing superhydrophobicity, exhibiting outstanding compressibility and stretchability among the reported counterparts.[31-39] In addition, the superhydrophobic coating also exhibited excellent anti-icing property. Because of versatile adhesion of PDA and simple synthesis process, the mussel-inspired strategy is extendable to fabricate mechanically durable superhydrophobic coatings on various elastic substrates desirable for many potential applications.

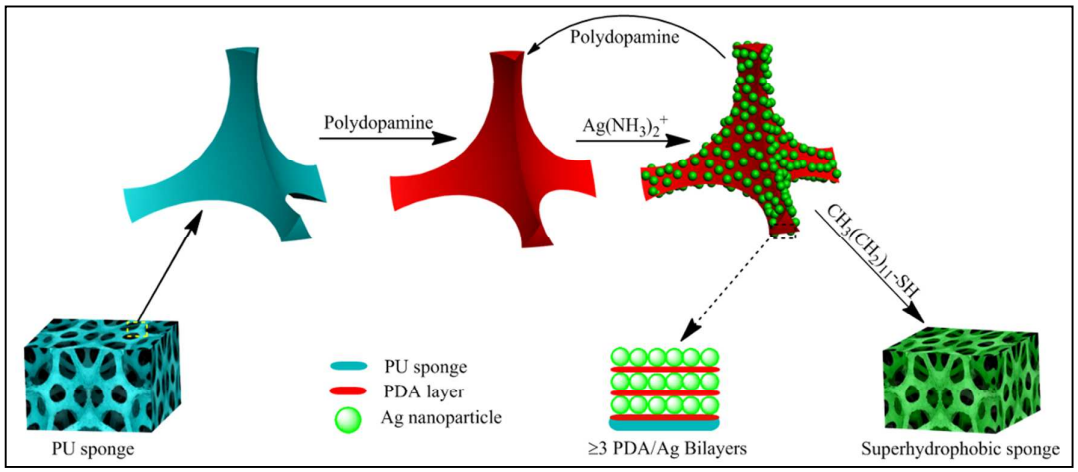

Scheme 1. Illustration for the fabrication of a highly compressible and stretchable superhydrophobic coating on PU sponge through layer-by-layer deposition.

2. Experimental

2.1 Materials and chemicals

Polyurethane (PU) sponge was purchased from Qingdao Yuquan sponge product Co. Ltd (China). Dopamine hydrochloride and tris(hydroxymethyl) aminomethane hydrochloride (Tris-HCl) were supplied by BASF Chemicals, Tianjin Co. Ltd (China). Silver nitrate ($AgNO_3$) was provided by Tianjin Benchmark Chemical Reagent Co. Ltd (China), and *n*-dodecanethiol (*n*-$C_{12}H_{25}SH$) was supplied by Tianjin Kermel Chemical Reagent Co. Ltd (China). All chemicals were used as received.

2.2 Preparation of superhydrophobic sponges through layer-by-layer deposition

In a typical experiment, a piece of PU sponge (1.0 cm × 1.0 cm × 0.8 cm in size) was added to a 10 mL of Tris-HCl buffer (10 mM, pH 8.5) containing dopamine (2 mg mL^{-1}). After being stirred for 30 min, the resulting sponge was washed with de-ionized water to obtain a PDA modified sponge. Then the PDA modified sponge was dipped in 30 mL of silver ammonia solution (5.9 mM) for 15 min to deposit Ag nanoparticles. After being washed with deionized water, the above processes were repeated for 1, 3, 5, and 7 cycles, respectively. At last, the resultant sponge was treated with 5 mM ethanol solution of *n*-dodecanethiol for 12 h at room temperature and dried at 60℃ in oven to obtain superhydrophobicity.

2.3 Preparation of superhydrophobic sponge by electroless deposition

A piece of PDA modified sponge was dipped in 30 mL of silver ammonia solution (5.9 mM), and then 17.5 mg of glucose was immediately added to the mixture. After being stirred for 15 min, the resulting sponge was successively washed with de-ionized water and ethanol. At last, the resultant sponge was treated with 5 mM ethanol solution of *n*-dodecanethiol for 12 h at room temperature and dried at 60℃ in oven to obtain superhydrophobicity.

Silver ammonia solution was prepared by slowly adding $NH_3 \cdot H_2O$ (25%) to 5 mL of aqueous solution of

$AgNO_3$ (35.4 mM) until the resulting solution became colorless. Then de-ionized water was added to the colorless solution until reaching a volume of 30 mL.

2.4 Anti-icing experiment

A piece of the pristine and superhydrophobic sponge (~2.4 mm in thickness) was separately fixed on a glass slide by adhesive tape. Then water droplets (7 μL) were dripped on the sponges and the slide was placed on a peltier cooling stage. After the temperature of the cooling stage was decreased to −15 ^{o}C, the icing process of the droplets was observed by a CCD camera and the delay time (DT) was measured. The room temperature was 17 ± 5 °C and the relative humidity was 45 ± 10%.

2.5 Characterizations

The morphologies of the sponges were observed by a FEI Quanta200 scanning electron microscope (SEM). X-ray photoelectron spectroscopy (XPS) measurement was conducted on a PHI-5700ESCA. The contact angles (CA) and hysteretic angles of the sponges were measured by an OCA20 (Dataphysics) using a droplet (3 μL) of water as indicator. Here, there was no distinct difference in contact angle when used a droplet of 3 or 5 μL. Cyclic compression measurements were performed on a universal electromechanical testing machine CMT 8102. In this study, the pristine and superhydrophobic sponges were successively compressed in X, Y, Z directions for a given number of cycles. X-ray diffraction (XRD) and transmission electron microscopy (TEM) measurements were conducted on an XRD-6000 (Shimadzu) and an H-7650 (Hitachi), respectively.

3. Results and discussion

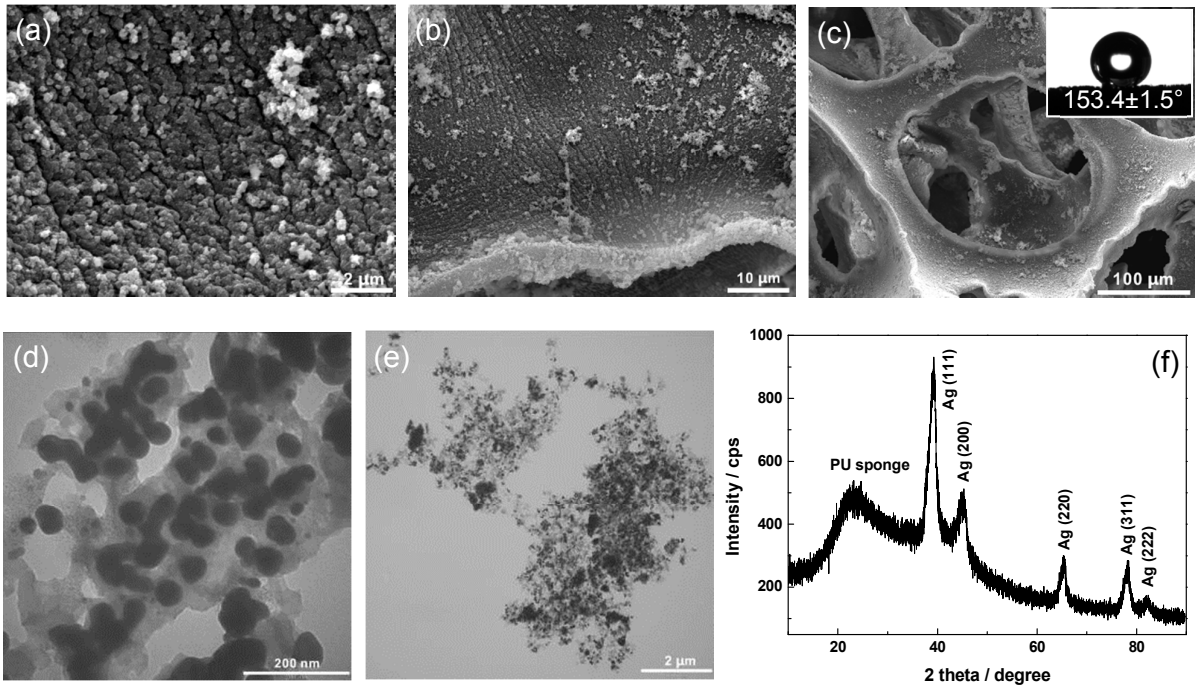

Fig. 1. SEM (a-c), TEM (d, e) and XRD pattern (f) images of superhydrophobic sponge with seven PDA/Ag bilayers; Inset was the water contact angle of the superhydrophobic sponge.

In this study, we used commercial PU sponges as elastic substrates to investigate the mechanical durability of a superhydrophobic coating. Ag nanoparticles were coated on the skeleton of PU sponge through the reduction of Ag^+ by polydopamine,[28,40] which provide roughness necessary for the superhydrophobic coating.[40,41] In addition, Ag nanoparticles can react with *n*-dodecanethiol to form thiolate,[42] reducing the surface energy of Ag nanoparticles. At first, the surface of PU sponges was coated with a polydopamine layer *via* self-polymerization of dopamine in Tris-HCl buffer at room temperature for 30 min (Fig. S1).[28,43,44] Then the resulting sponges were successively treated with silver ammonia and dopamine/Tris-HCl solutions to deposit PDA/Ag bilayer. This layer-by-layer deposition process was repeated for 7 times. After modification with *n*-dodecanethiol, the sponges exhibited water contact angles of 153.4 ± 1.5^o and hysteretic angles 2.7 ± 1^o.

The chemical composition and morphology of a typical superhydrophobic sponge were characterized by XRD,

SEM and TEM measurements. XRD pattern together with SEM images show that Ag nanoparticles of 50-100 nm evenly cover on the skeleton of the sponge, forming a porous appearance (Fig. 1a-c and Fig. 1f). Notably, isolated clusters with micron size are also observed on the coating, which were formed in solutions and then deposited onto the skeleton under the gravity force (Fig. 1c). TEM images illustrate that Ag nanoparticles have a diameter of ~60 nm and they homogeneously distribute on the surface of PDA layer (Fig. 1d-e).

The morphology and wettability of the resulting coatings were strongly dependent on the number of PDA/Ag bilayers (Fig. 1b-c, and Fig. S2). The coatings increase their surface roughness as the number of PDA/Ag bilayers is increased from 1 to 7. Similar trend is also observed for the water contact angles of the coatings. For instance, a coating shows CA of 149° as its bilayers number is only one, while the value increases to 153.4° for the coating containing seven PDA/Ag bilayers (Fig. S3a). In contrast, the coatings decrease their hysteretic angles when the number of PDA/Ag bilayers is increased from 1 to 7 (Fig. S3b). These results suggest that increasing the number of PDA/Ag bilayers is beneficial for the formation of a superhydrophobic coating with large CA and low hysteretic angle. Recently, Xu *et al*[40] fabricated a family of superhydrophobic particles by using polydopamine as interlayer, but this strategy was rarely applied to a monolithic substrate. Therefore, the above results demonstrate the possibility of fabricating a superhydrophobic coating on monolithic porous substrates by using PDA as interlayers.

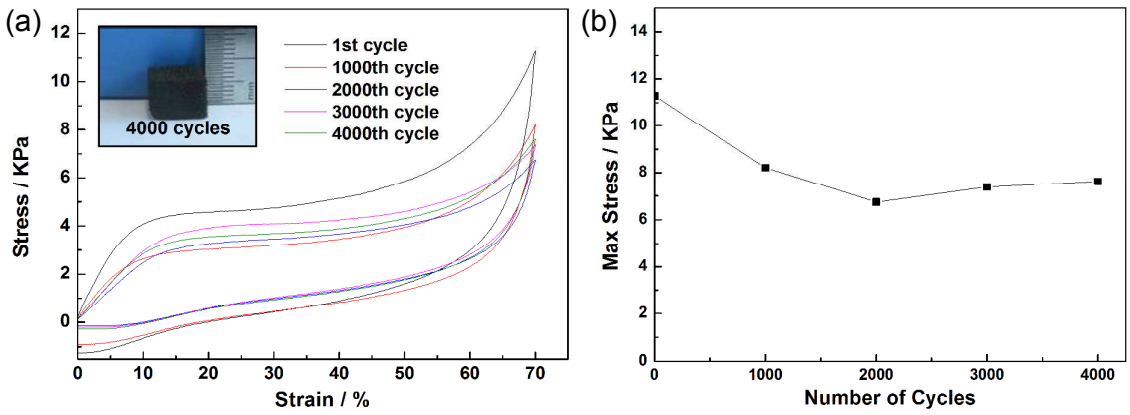

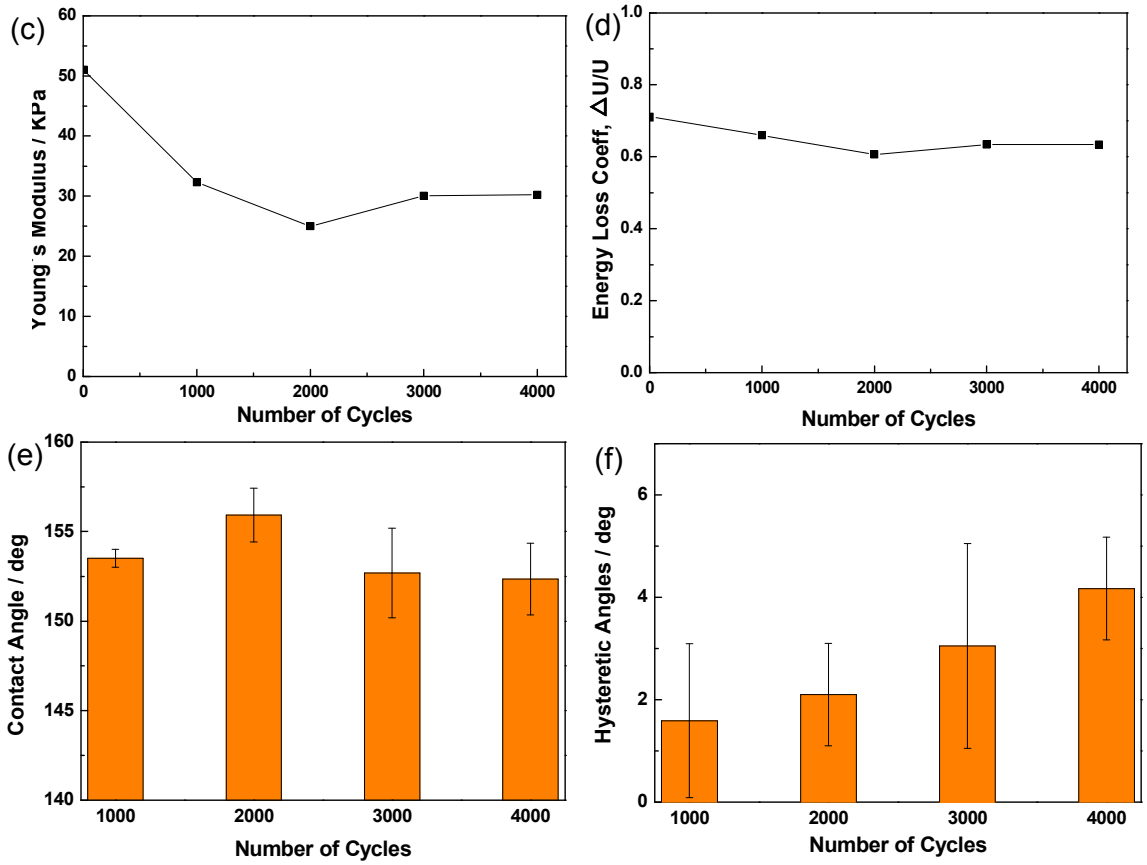

Fig. 2. (a) Stress-strain curves of the superhydrophobic sponge in compression processes with a maximum strain of 70% at a loading rate of 10 mm min^{-1}. (b) Change of the maximum stress, (c) Young's modulus and (d) energy loss coefficient with compression cycles. Variation of the contact angles (e) and hysteretic angles (f) of the sponge with compression cycles. Inset is the optical image of the sponge after 4000-cycle compression.

Then the mechanical durability of the superhydrophobic coating (with seven PDA/Ag bilayers) was investigated by cyclic compression and tensile tests. Cyclic compression measurements revealed that the superhydrophobic coating was highly compressible even at a strain up to 70%. Fig. 2a shows typical stress-strain curves of the sponge at the maximum strain of 70%. The curves exhibit three stages at $\varepsilon < 10\%$, $10\% < \varepsilon < 50\%$ and $\varepsilon > 50\%$, corresponding to the elastic, the plateau and the densification regions, respectively.[45] The elastic region showing a modulus ~51.0 KPa indicates the elastic bending of the sponge skeleton, while the plateau region suggests the recoverable deformation of the skeleton. A rapid increase in stress is observed at $\varepsilon > 50\%$,

indicating continuously decreased pore volume of the sponge. After the finish of each compression cycle, a hysteresis loop appears, implying the dissipation of mechanical energy. Although the loop shrinks continuously in the subsequent compression process,[46] the stress-strain curve of the 4000th cycle is similar to that of the 1st cycle except the decreased maximum stress. Fig. 2b-d presents the maximum stress, energy loss coefficient and Young's modulus in the compression process. They decrease continuously after the first cycle, and reach 67.5, 89.2 and 59.2% of the initial values after 4000 cycles, respectively. In contrast, Young's modulus drops more significantly compared with the maximum stress and energy loss coefficient. We also measured the stress-strain curves of a pristine sponge (Fig. S4), it showed similar mechanical properties as the superhydrophobic counterpart, suggesting that the superhydrophobic coating did not significantly affect the elasticity of the sponge. Indeed, the superhydrophobic sponge kept its original volume and cellular structure after continuous compressions for 4000 cycles, indicating that it was able to withstand a large-strain deformation without fracture or collapse (Inset of Fig. 2a).

The high compressibility of the superhydrophobic coating was further confirmed by the variation of water contact angle and hysteretic angle in the compression process. The sponge shows water contact angles all above 150^{o} in the process (Fig. 2e), indicating it can withstand at least 4000 cycles of large-strain compressive deformation without losing superhydrophobicity. Nevertheless, its hysteretic angles increase slightly in the compression process (Fig. 2f). Even after 6000-cycle compression, the sponge still exhibits a water contact angle of 152.4 ± 1° and a hysteretic angle of 5.5 ± 3^{o}, implying the excellent durability of the superhydrophobic coating.

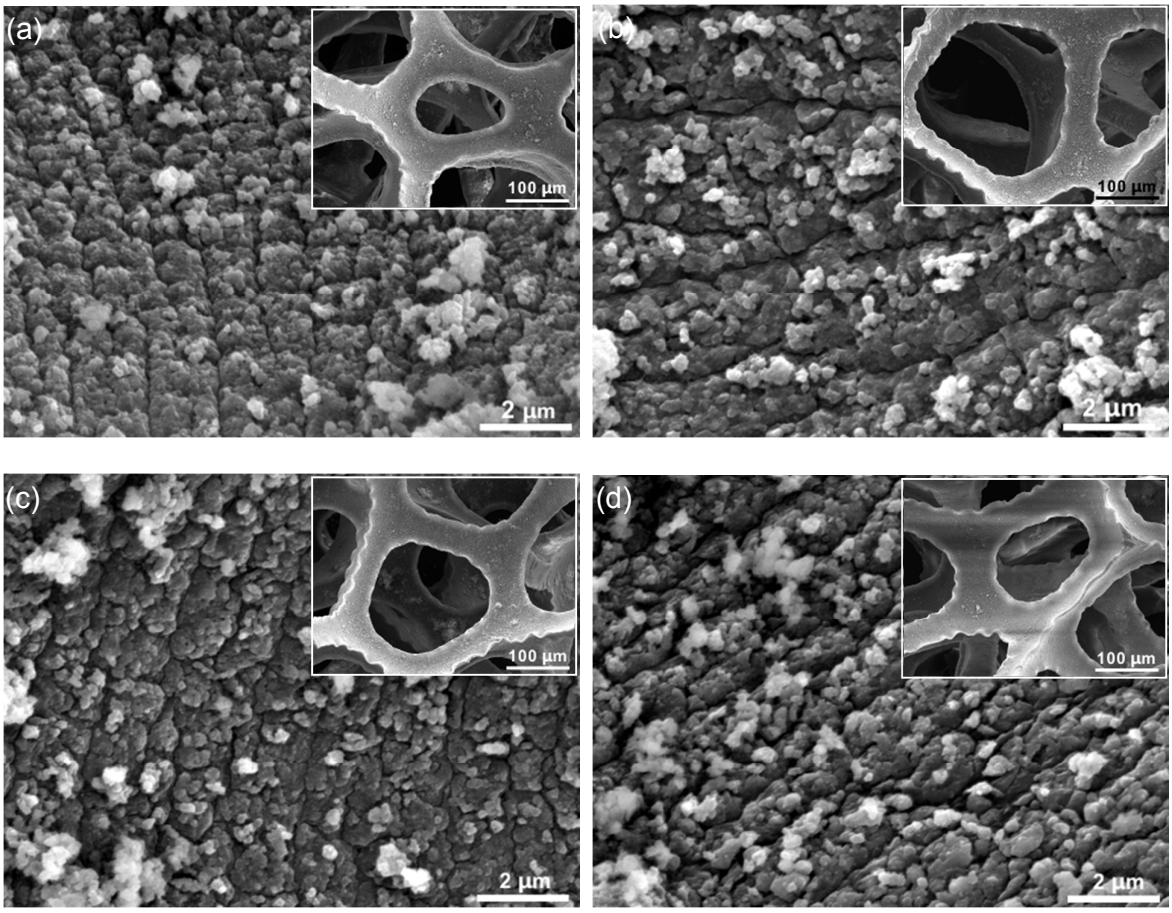

Fig. 3. SEM images of the superhydrophobic coating after compression for (a) 1000 cycles, (b) 2000 cycles, (c) 3000 cycles, (d) 4000 cycles.

The evolution of surface morphology in the compression process provided another evidence for the high compressibility of the superhydrophobic coating. SEM images in Fig. 3 show that Ag nanoparticles still homogeneously cover on the sponge's surface after the 4000-cycle compression test, indicating good adhesion between Ag nanoparticles, polydopamine layers and sponge skeletons. Compared with the morphology before compression (Fig. 1a), however, cracks on the coating become wider in the compression process, forming a more porous appearance after compression for 4000 cycles (Fig. 3d). The widening of the cracks is due to the detachment of a small part of Ag nanoparticles from the coating by the compressive stress. It is believed that these cracks can act as "buffering regions" for the bending deformation of the coating. As a result, Ag nanoparticles still

homogeneously cover on the sponge's surface even after 6000-cycle compression (Fig. S5). We also compared the present sponge with other reported superhydrophobic counterparts,[3-6,9-11,13,31-39] and found that it showed outstanding compressibility. All these results demonstrate excellent compressibility of the superhydrophobic coating on the sponge.

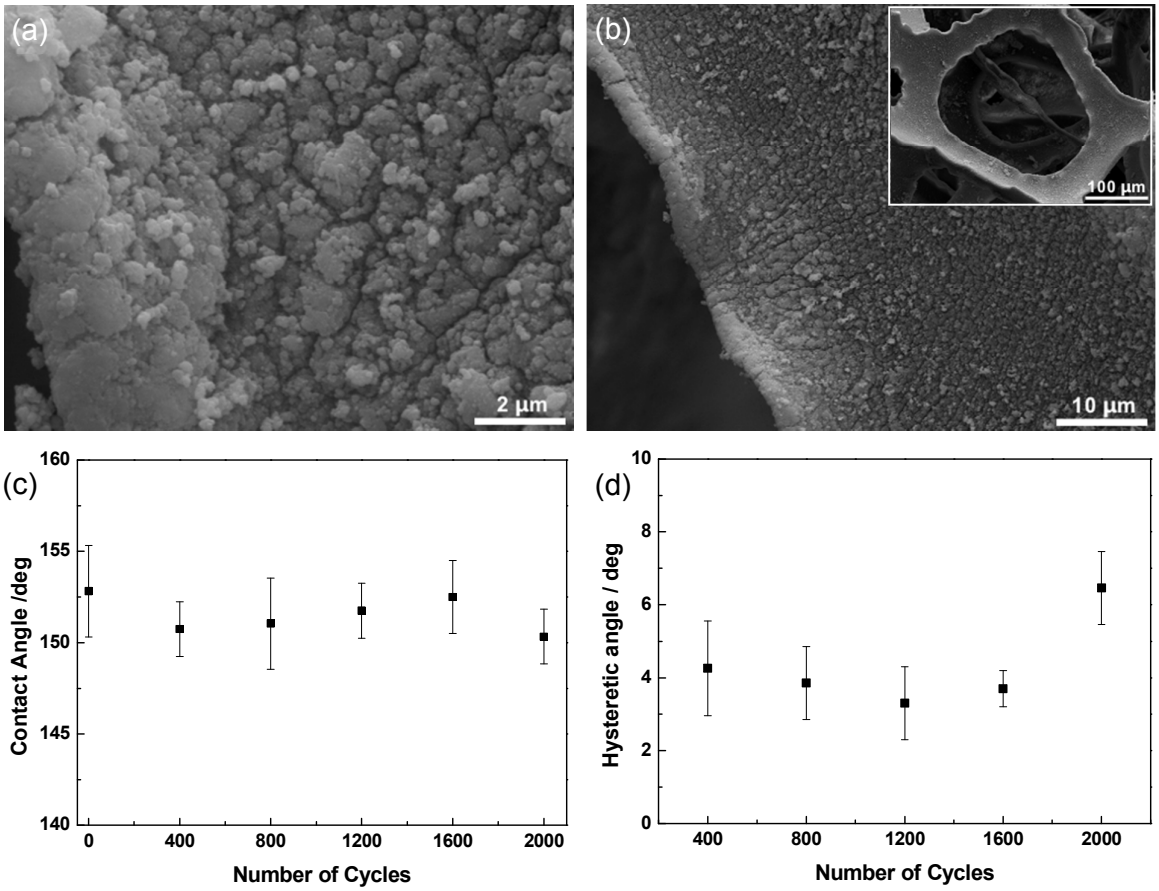

Fig. 4. (a, b) SEM images of the superhydrophobic coating after stretching for 2000 cycles, tensile strain ε = 40%. Variation of the contact angles (c) and hysteretic angles (d) of the superhydrophobic sponge in the tensile process. The size of superhydrophobic sponge is 2.5 cm × 1.0 cm × 0.8 cm in the tensile test.

Another characteristic of the coating is high stretchability. In a typical tensile test, the superhydrophobic sponge was stretched to a strain of 40%, and then it was relaxed to recover shape. SEM images reveal that cracks developed in the tensile process, but Ag nanoparticles still homogeneously cover on the sponge's surface (Fig. 4a-b), suggesting excellent durability of the superhydrophobic coating against drawing force. After 2000 cycles of

stretching, the sponge maintained superhydrophobicity because it still exhibited a water contact of 150.3 ± 1.5° and a hysteretic angle of 6.46 ± 1° (Fig. 4c-d). Notably, although many studies used polydopamine for surface modification and material synthesis, its mechanical properties on different substrates were rarely investigated.[43,44] Therefore, the above results not only provide a facile method for fabricating a robust superhydrophobic coating on PU sponges, but also investigate the mechanical durability of a polydopamine layer.

The high mechanical durability of the superhydrophobic coating is believed to originate from the reinforcement effect of PDA interlayers on Ag nanoparticles. To investigate this speculation, Ag nanoparticles were directly deposited on a PDA-modified PU sponge through an electroless deposition, without further coating with a PDA layer. After the treatment with *n*-dodecanethiol, the sponge was tested by cyclic compression and its surface morphology, contact angle and hysteretic angle were recorded. The obtained SEM images (Fig. S6a-d) show significant detachment of Ag nanopartiles from the surface of the sponge after 4000-cycle compression, forming a contrast to the superhydrophobic coating having a sandwich-like structure. The water contact angle of the sponge also decreases from 152.3 ± 1° to 142.3 ± 5° (Fig. S6e). Moreover, its hysteretic angle increases from 3.8 ± 1.5° to 10.9 ± 2.5° (Fig. S6f). These results reveal that sandwich-like PDA/Ag/PDA multilayers play an important role in the mechanical durability of superhydrophobic coatings. In other words, PDA interlayers have a reinforcement effect on Ag nanoparticles.

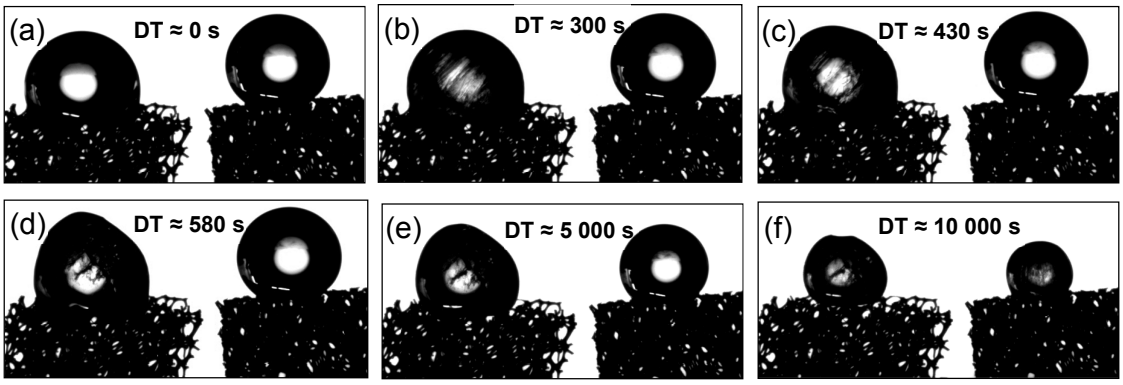

Fig. 5. Icing process of water droplets on the pristine sponge (left) and superhydrophobic sponge (right) at –15 °C.

Besides durable superhydrophobicity, the coating also exhibited excellent anti-icing property. To investigate this characteristic, we used a CCD camera to observe the icing process of a water droplet (7 μL) on the as-prepared sponge at −15 ^{o}C (Fig. 5). For comparison, the same process was also performed on a pristine sponge. Under the same conditions, the superhydrophobic sponge exhibited a better anti-icing performance than the pristine counterpart. For example, the droplet started to freeze on the pritine sponge at the delay time (DT) of ~300 s, while that on the superhydrophobic sponge freezed after DT ~10000 s. These results were comparable with those reported superhydrophobic surfaces.[20,47-49] The excellent anti-icing performance originates from the hierarchical porous structures (*i.e.*, micrometer macropore and nanoscale pore) of the superhydrophobic sponge.[50] These hierarchical structures slow dowm the heat condution between water droplets and the cooling stage to some extent, which confers icephobic properties of the superhydrophobic sponge.

On the basis of above results, we propose possible reasons for the high compressibility and stretchability of the superydrophobic coating. At first, polydopamine layer strongly adheres to the sponge skeleton, providing a robust underlayer[51] for Ag nanoparticles. The strong adhesion is related to covalent binding and noncovalent interfacial interactions between the polydopamine layer and the sponge skeleton.[28,43,44] The former arises from Michael addition or Shiff base substitution between –NH– group of the PU skeleton and *o*-quinone functionality of the polydopamine layer,[52] while the later includes hydrogen bonding, π-π interactions, and electrostatic interactions, *etc*. More importantly, the strong adhesion also enhances the mechanical stability of Ag nanoparticles embedded in the adjacent PDA layers. Second, XPS results showed that Ag nanoparticles have chemical interactions with polydopamine interlayers (Fig. S7). Generally, strong adhesion between metal and polymer is difficult to achieve due to different surface energies. However, metal-polymer adhesion is significantly improved by introducing polar functionalities like C=O and C–N to polymer.[53-56] Since polydopamine layers contain C–N, C=O, and –OH,[43,44] interactions with these functionalities improve the mechanical durability of Ag nanoparticles against the

external stress. All these factors ensure high compressibility and stretchability of the superhydrophobic coating.

4. Conclusions

In summary, taking inspiration from the adhesive properties of catecholic moieties, we fabricated a highly compressible (≥ 6000 cycles) and stretchable (≥ 2000 cycles) superhydrophobic coating on commercial PU sponges through layer-by-layer deposition, which was not accessible by traditional methods. The coating exhibited not only good mechanical durability but also excellent anti-icing performance. Although the mechanism for the outstanding mechanical durability deserves further investigations, it is believed that the strong interactions (or adhesion) between Ag nanoparticles, PDA interlayers and PU sponge skeleton make the sandwich-like superhydrophobic coating insensitive to the compressive stress and tension. Because of strong adhesion of polydopamine to a wide range of substances and simple synthesis process, the results of this study offer a facile and versatile strategy for fabricating a mechanically robust coating on various elastic substrates desirable for oil-water separation, energy cushion, antibacterial surface, and electrostatic shielding, *etc*.

References

1 X. Yao, Y. L. Song and L. Jiang, *Adv. Mater.*, 2011, **23**, 719.

2 Y. Zhang, Y. Chen, L. Shi, J. Li and Z. Guo, *J. Mater. Chem.*, 2012, **22**, 799.

3 C. H. Xue and J. Z. Ma, *J. Mater. Chem. A*, 2013, **1**, 4146.

4 D. Quéré, *Annu. Rev. Mater. Res.*, 2008, **38**, 71.

5 J. T. Han, Y. Zheng, J. H. Cho, X. Xu and K. Cho, *J. Phys. Chem. B*, 2005, **109**, 20773.

6 T. Verho, C. Bower, P. Andrew, S. Franssila, O. Ikkala and R. H. A. Ras, *Adv. Mater.*, 2011, **23**, 673.

7 J. Groten and J. Rühe, *Langmuir*, 2013, **29**, 3765.

8 B. C. Li, J. P. Zhang, L. Wu and A. Q. Wang, *Chempluschem*, 2013, **78**, 1503.

9 J. Zimmermann, F. A. Reifler, G. Fortunato, L. C. Gerhardt and S. Seeger, *Adv. Funct. Mater.*, 2008, **18**, 3662.

10 B. Deng, R. Cai, Y. Yu, H. Jiang, C. Wang, J. Li, L. Li, M. Yu, J. Li, L. Xie, Q. Huang and C. Fan, *Adv. Mater.*, 2010, **22**, 5473.

11 X. Deng, L. Mammen, Y. Zhao, P. Lellig, K. Mullen, C. Li, H. J. Butt and D. Vollmer, *Adv. Mater.*, 2011, **23**, 2962.

12 L. Wu, J. P. Zhang, B. C. Li and A. Q. Wang, *Polym. Chem.*, 2014, **5**, 2382.

13 H. Zhou, H. Wang, H. Niu, A. Gestos, X. Wang and T. Lin, *Adv. Mater.*, 2012, **24**, 2409.

14 E. Huovinen, L. Takkunen, T. Korpela, M. Suvanto, T. Pakkanen and T. Pakkanen, *Langmuir*, 2014, **30**, 1435.

15 H. Wang, Y. Xue, J. Ding, L. Feng, X. Wang and T. Lin, *Angew. Chem., Int. Ed.*, 2011, **50**, 11433.

16 Y. Li, L. Li and J. Sun, *Angew. Chem., Int. Ed.*, 2010, **49**, 6129.

17 X. Wang, X. Liu, F. Zhou and W. Liu, *Chem. Commun.*, 2011, **47**, 2324.

18 L. Ionov and A. Synytska, *Phys. Chem. Chem. Phys.*, 2012, **14**, 10497.

19 U. Manna, M. C. D. Carter and D. M. Lynn, *Adv. Mater.*, 2013, **25**, 3085.

20 S. A. Kulinich, S. Farhadi, K. Nose and X. W. Du, *Langmuir*, 2011, **27**, 25.

21 S. Farhadi, M, Farzaneh and S. A. Kulinich, *Appl. Surf. Sci.*, 2011, **257**, 6264.

22 Y. Y. Wang, J. Xue, Q. J. Wang, Q. M. Chen and J. F. Ding, *ACS Appl. Mater. Interfaces*, 2013, **5**, 3370.

23 J. H. Waite and M. L. Tanzer, *Science*, 1981, **212**, 1038.

24 H. G. Silverman and F. F. Roberto, *Mar. Biotechnol.*, 2007, **9**, 661.

25 H. Lee, N. F. Scherer and P. B. Messersmith, *Proc. Natl. Acad. Sci. U. S. A.*, 2006, **103**, 12999.

26 J. H. Waite, R. A. Jensen and D. E. Morse, *Biochemistry*, 1992, **31**, 5733.

27 J. H. Waite, *Integr. Comp. Biol.*, 2002, **42**, 1172.

28 L. Haeshin, S. M. Dellatore, W. M. Miller and P. B. Messersmith, *Science*, 2007, **318**, 426.

29 Q. F. Cheng, L. Jiang and Z. Y. Tang, *Acc. Chem. Res.*, 2014, **47**, 1256.

30 Q. F. Cheng, M. X. Wu, M. Z. Li, L. Jiang and Z. Y. Tang, *Angew. Chem., Int. Ed.* 2013, **52**, 3750.

31 X. Y. Zhang, Z. Li, K. S. Liu and L. Jiang, *Adv. Funct. Mater.*, 2013, **23**, 2881.

32 Q. Zhu and Q. Pan, *ACS Nano*, 2014, **8**, 1402.

33 Q. Zhu, Q. Pan and F. Liu, *J. Phys. Chem. C*, 2011, **115**, 17464.

34 X. C. Gui, Z. P. Zeng, Z. Q. Lin, Q. M. Gan, R. Xiang, Y. Zhu, A. Y. Cao and Z. K. Tang, *ACS Appl. Mater. Interfaces*, 2013, **5**, 5845.

35 A. Li, H. X. Sun, D. Z. Tan, W. J. Fan, S. H. Wen, X. J. Qing, G. X. Li, S. Y. Li and W. Q. Deng. *Energy Environ. Sci.*, 2011, **4**, 2062.

36 Q. Zhu, Y. Chu, Z. Wang, N. Chen, L. Lin, F. Liu and Q. Pan, *J. Mater. Chem. A*, 2013, **1**, 5386.

37 B. Wang, J. Li, G. Y. Wang, W. X. Liang, Y. B. Zhang, L. Shi, Z. G. Guo and W. M. Liu, *ACS Appl. Mater. Interfaces*, 2013, **5**, 1827.

38 P. Calcagnile, D. Fragouli, I. S. Bayer, G. C. Anyfantis, L. Martiradonna, P. D. Cozzoli, R. Cingolani and A.

Athanassiou, *ACS Nano*, 2012, **6**, 5413.

39X. C. Dong, J. Chen, Y. W. Ma, J. Wang, M. B. Chan-Park, X. M. Liu, L. H. Wang, W. Huang and P. Chen, *Chem. Commun.*, 2012, **48**, 10660.

40 L. Zhang, J. Wu, Y. Wang, Y. Long, N. Zhao and J. Xu, *J. Am. Chem. Soc.*, 2012, **134**, 9879.

41 K. S. Liu and L. Jiang, *Nano Today*, 2011, **6**, 155.

42 Y. Zhao, Q. H. Lu, D. S. Chen and Y. Wei, *J. Mater. Chem.*, 2006, **16**, 4504.

43 Q. Ye, F. Zhou and W. Liu, *Chem. Soc. Rev.*, 2011, **40**, 4244.

44 J. Sedó, J. Saiz-Poseu, F. Busqué and D. Ruiz-Molina, *Adv. Mater.*, 2013, **25**, 653.

45 H. Hu, Z. B. Zhao, W. B. Wan, Y. Gogotsi and J. S. Qiu, *Adv. Mater.*, 2013, **25**, 2219.

46 J. Suhr, P. Victor, L. Ci, S. Sreekala, X. Zhang, O. Nalamasu and P. Ajayan, *Nat. Nanotechnol.*, 2007, **2**, 417.

47 P. Guo, Y. M. Zheng, M. X. Wen, C. Song, Y. C. Lin and L. Jiang, *Adv. Mater.*, 2012, **24**, 2642.

48 M. Nosonovsky and V. Hejazi, *ACS Nano*, 2012, **6**, 8488.

49 J. Lv, Y. Song, L. Jiang, and J. Wang, *ACS Nano*, 2014, **8**, 3152.

50 C. Y. Peng, S. L. Xing, Z. Q. Yuan, J. Y. Xiao, C. Q. Wang and J. C. Zeng, *App. Surf. Sci.*, 2012, **259**, 764.

51 J. F. Ou, J. Q. Wang, S. Liu, J. F. Zhou and S. R. Yang, *J. Phys. Chem. C*, 2009, **113**, 20429.

52 J. Saiz-Poseu, J. Sedó, B.García, C. Benaiges, T. Parella, R. Alibés, J. Hernando, F. Busqué and D. Ruiz-Molina, *Adv. Mater.*, 2013, **25**, 2066.

53 S. Serghini-Monim, P. R. Norton, R. J. Puddephatt, K. D. Pollard and J. R. Rasmussen, *J. Phys. Chem. B*, 1998, **102**, 1450.

54 L. J. Gerenser, *J. Vac. Sci. Technol. A*, 1990, **8**, 3682.

55 L. J. Gerenser, *J. Vac. Sci. Technol. A*, 1988, **6**, 2897.

56 J. E. Gray, T, P. R. Nortonb and K. Griffiths, *Thin Solid Films*, 2005, **484**, 196.

TOC

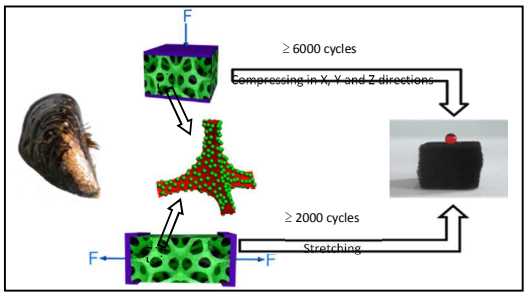

A highly compressible and stretchable superhydrophobic coating was fabricated by layer-by-layer deposition of Ag nanoparticles and polydopamine.